JOURNAL OF MATERIALS SCIENCE 22 (1987) 3595–3601

In situ measurement of silicon oxidation kinetics by monitoring spectrally emitted radiation

GERHARD H. SCHIROKY*
GA Technologies, Inc., John Jay Hopkins Drive, San Diego, California 92121, USA

When a highly polished silicon wafer is thermally oxidized, its spectral emittance fluctuates systematically, as the protective silica film grows thicker. If the spectral intensity of the emitted radiation at a wavelength where silica is transparent is monitored, the film thickness can be obtained.

1. Introduction

The oxidation of silicon has been investigated in numerous studies, and presented in a large number of publications. Only a very few are listed here [1–9], which should serve as a guide to further references. The thickness of the silica film; which forms during oxidation on the silicon surface, was measured in nearly all studies after completion of the experiment. The preferred measurement technique has been ellipsometry, as it provides excellent film thickness resolution. This technique can be adapted for *in situ* measurements as well [10, 11]. It is the purpose of this publication to introduce a novel method with which silicon oxidation can be followed optically in a rather simple way. The principle of this method is to monitor the spectral thermal radiation emitted by a polished silicon wafer at a wavelength at which the silica film is fully transparent. The interference conditions within the film change as it becomes thicker, and thus lead to fluctuations in the emitted radiation intensity. From these, the growth kinetics can be determined. The advantages and limitations of this method are discussed.

2. Theory

As most materials scientists do not get involved in optics, a rather detailed explanation of the theory underlying the optical measurement technique is presented. The reader is referred to traditional textbooks on optics [12] for additional discussion of basic principles.

An expression will be given for the spectral intensity of electromagnetic radiation emitted in the normal direction from an absorbing substrate with a thin transparent film. Due to the restriction to normal emission one does not have to deal with the directional dependence of the optical properties of absorbing substrates. Experimentally it is easier to measure normal intensities only. It is assumed that the surfaces of substrate and film are optically smooth, and that the film is uniform in thickness. The term "thin film" refers generally to a film thickness of a few hundred nanometers.

A graphic representation of the system substrate–film–environment is shown in Fig. 1. The (real) refractive indexes of the media are denoted n_1, n_2, and n_3, respectively, while k_3 is the absorption coefficient of the substrate. Thus, $n_3^* = n_3 + ik_3$ stands for the complex refractive index of the substrate. The parameters r_{12} and r_{23} are the Fresnel coefficients for the film/air and film/substrate interface, respectively. They can be calculated from the relations:

$$r_{12} = \frac{n_1 - n_2}{n_1 + n_2} \tag{1}$$

and

$$r_{23}^2 = \frac{(n_2 - n_3)^2 + k_3^2}{(n_3 + n_2)^2 + k_3^2} \tag{2}$$

From Equation 1 it follows for an air/glass interface that $r_{12} < 0$. This means that an incoming electromagnetic wave experiences a phase change of π upon reflection at the glass surface. A phase shift β_{23} occurs at the film/substrate interface:

$$\tan \beta_{23} = \frac{2n_2k_3}{n_3^2 - n_2^2 + k_3^2} \tag{3}$$

The sign of r_{23} and quadrant of $\tan \beta_{23}$ can be readily evaluated. Comparison of the real and imaginary parts of Equation 4 and 5

$$r_{23}e^{i\beta_{23}} = \frac{n_2 - n_3^*}{n_2 + n_3^*} = \frac{n_2^2 - n_3^2 - k_3^2}{(n_2 + n_3)^2 + k_3^2} + i\frac{(-2n_2k_3)}{(n_2 + n_3)^2 + k_3^2} \tag{4}$$

$$r_{23}e^{i\beta_{23}} = r_{23}\cos\beta_{23} + ir_{23}\sin\beta_{23} \tag{5}$$

suggests that for $r_{23} > 0$, $\pi < \beta_{23} < 2\pi$. As it is more convenient to operate with smaller angles, we take $r_{23} < 0$ and $0 < \beta_{23} < \pi$.

The monochromatic specular reflectance of an absorbing substrate with a transparent film (see Appendix A for a derivation) is

$$R = \frac{r_{12}^2 + r_{23}^2 + 2r_{12}r_{23}\cos(\beta_{23} + \alpha)}{1 + r_{12}^2r_{23}^2 + 2r_{12}r_{23}\cos(\beta_{23} + \alpha)} \tag{6}$$

*Present address: Lanxide Corporation, Tralee Industrial Park, Newark, Delaware 19711, USA.

0022–2461/87 $03.00 + .12

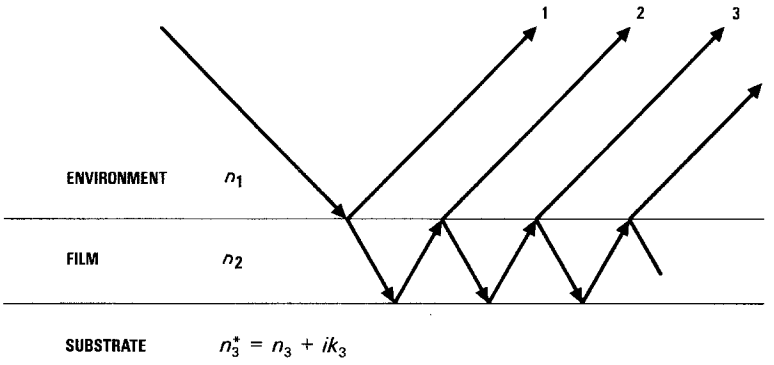

Figure 1 The optical constants in the investigated system.

The term α is the phase shift between the waves 1 and 2, 2 and 3, etc, (Fig. 1), due to the optical path difference between these waves in the film. For normal incidence, the path difference is simply twice the film thickness d, so that

$$\alpha = \frac{4\pi d n_2}{\lambda} \tag{7}$$

where λ denotes the free space wavelength. The factor n_2 enters this expression for α as the wavelength within the film equals λ/n_2.

Equations 1 and 4 are for perpendicular polarized radiation. As for normal incidence the difference between perpendicular and parallel polarized radiation disappears, the equations for the parallel case could have been used here as well. Equation 6 pertains to both cases.

For the system shown in Fig. 1, one can draw an energy balance and write the incident flux as the sum of the reflected, absorbed, and transmitted fluxes. Normalizing the latter three with respect to the incident flux yields

$$R + A + T = 1 \tag{8}$$

with R, A, and T as reflectance, absorptance, and transmittance, respectively. In our case, the substrates are thick enough so that $T = 0$. Hence,

$$R + A = 1 \tag{9}$$

According to Kirchhoff's law, the emittance E equals the absorptance,

$$E = A \tag{10}$$

so that, with Equation 9

$$E = 1 - R \tag{11}$$

Kirchhoff's law is derived in many texts for thermodynamic equilibrium, i.e., for systems uniform in all state variables and hence no net radiative transport. There is, however, ample experimental evidence that Kirchhoff's law also holds well in situations with net transfer as long as the gradients are not so steep that the local equilibrium concept is jeopardized. This implies that the population of energy states participating in the absorption and emission processes must still be well approximated by their thermal equilibrium distribution.

According to Equations 6 and 11 the emittance of an absorbing substrate with a transparent film is given by

$$E = \frac{1 - r_{12}^2 + r_{12}^2 r_{23}^2 - r_{23}^2}{1 + r_{12}^2 r_{23}^2 + 2 r_{12} r_{23} \cos(\beta_{23} + \alpha)} \tag{12}$$

For an alternate, more fundamental derivation of Equation 12, see Appendix A. For the specific example of a silica film on a silicon substrate the normal spectral emittance at $\lambda = 694.3\,\text{nm}$ and $T = 1300°\,\text{C}$ is plotted as a function of silica film thickness in Fig. 2. Note, that as the film thickness approaches zero, the emittance is the same as from a clean substrate without a film.

The $E(d)$ curve is a function of temperature, as the optical constants of silicon and SiO_2 are temperature dependent. The optical constants of silica can be estimated with reasonable accuracy. Measurements of the refractive index of fused silica [13] between 26 and 828° C for wavelengths between 230 and 3370 nm showed that n_{SiO_2} displays a very weak temperature dependence only. Linear extrapolation of the data yields n_{SiO_2} (1300° C, 694.3 nm) = 1.47. For comparison, n_{SiO_2} (26° C, 694.3 nm) = 1.457. Other investigations [10, 11] showed, that at least up to 1100° C,

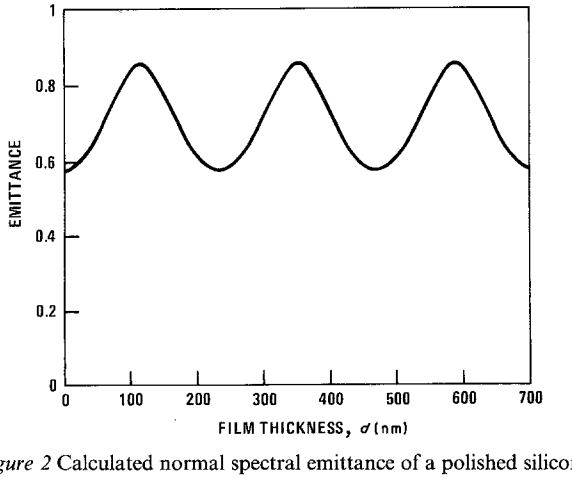

Figure 2 Calculated normal spectral emittance of a polished silicon wafer as a function of silica film thickness for $\lambda = 694.3\,\text{nm}$ and $T = 1300°\,\text{C}$.

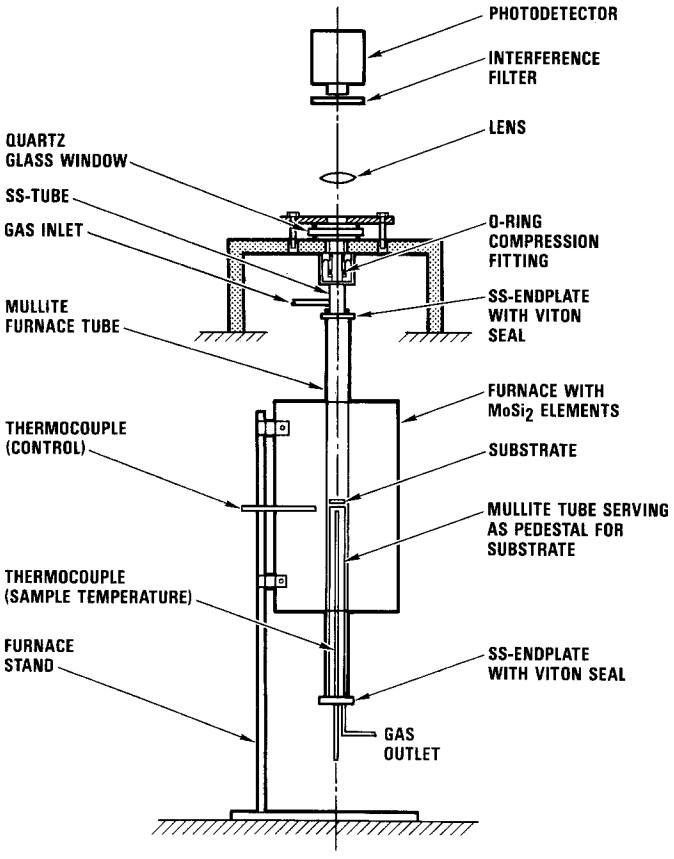

Figure 3 Experimental setup.

the silica films remained fully transparent for $\lambda = 632.8$ nm. Hence, our assumption that k_{SiO_2} (1300° C, 694.3 nm) = 0.0 is not unreasonable.

As a result of *in situ* growth rate measurements with ellipsometry [10, 11] the temperature dependence of n_{Si} and k_{Si} at $\lambda = 632.8$ nm have become available. The extrapolation of $n_{Si}(T)$ to 1300° C can be carried out with good accuracy. One obtains n_{Si} (1300° C, 632.8 nm) = 4.5 ± 0.1. An extrapolated value of k_{Si} (1300° C, 632.8 nm) of 1.0 should be considered a tentative guess. This compares to room temperature values at 632.8 nm of 3.88 for n_{Si} and 0.02 for k_{Si}. To complicate matters even more, n_{Si} and k_{Si} depend on wavelength, too. For a plot of $n_{Si}(\lambda)$ and $k_{Si}(\lambda)$, see [14]. As a first order approximation, we assumed for the $E(d)$ plot in Fig. 2 that n_{Si} (694.3 nm, 1300° C) = n_{Si} (632.8 nm, 1300° C), and k_{Si} (694.3 nm, 1300° C) = k_{Si} (632.8 nm, 1300° C).

With the optical constants from above, one obtains with Equation 3 that $\beta_{23} = 8.8°$. This phase shift has the same influence on emittance as a film of thickness 5.7 nm, as calculated from Equations 6 and 7. Therefore, there is no minimum in the $E(d)$-curve in Fig. 2 at $d = 0$, but rather at $d = -5.7$ nm.

The intensity I of the emitted normal spectral radiation is proportional to E. Hence, if one oxidizes an initially bare silicon substrate, and records I as a function of time t, one obtains a curve with fluctuating amplitude. From the extrema in the recorded $I(t)$-curve one can readily establish a $d(t)$-curve with Equation 12. For $\beta_{23} + \alpha = 2m\pi$ ($m = 0, 1, 2, 3 \ldots$), E, and hence I, is a minimum, i.e., with Equation 7, minima in $I(t)$ occur for

$$d_{min} = (2m\pi - \beta_{23}) \frac{\lambda}{4\pi n_2} \quad (13)$$

and, similarly, maxima for

$$d_{max} = [(2m + 1)\pi - \beta_{23}] \frac{\lambda}{4\pi n_2} \quad (14)$$

For a small enough β_{23}, Equations 13 and 14 reduce to

$$d_{min} = \frac{m\lambda}{2n_2} \quad (15)$$

and

$$d_{max} = (2m + 1) \frac{\lambda}{4n_2} \quad (16)$$

3. Experimental procedure

A schematic of the experimental setup is shown in Fig. 3. The sample, a polished (1 1 1)-oriented silicon wafer, is supported by a mullite tube within the mullite furnace tube, so that the optical axis of the setup is perpendicular to the sample surface. The sample temperature is measured with a B-type thermocouple at a distance less than 20 mm from its rear face. A lens with a focal length of 400 mm is used to project the radiation from a small spot on the sample onto a silicon photodetector diode. Both image and object distance are 800 mm (1 : 1 optics). An interference filter with 50% peak transmittance at 694.3 nm (ruby laser line) and a full width at half maximum of 10 nm is positioned in front of the detector. Considering the small dimension of the photodiode (2 mm diameter) and the large image distance, the transmittance spectrum shift of the filter to lower wavelength for non-normal incidence is completely negligible.

With a sample placed on the pedestal, the furnace tube was evacuated with a mechanical pump and heated under vacuum to 600° C, where it was held for

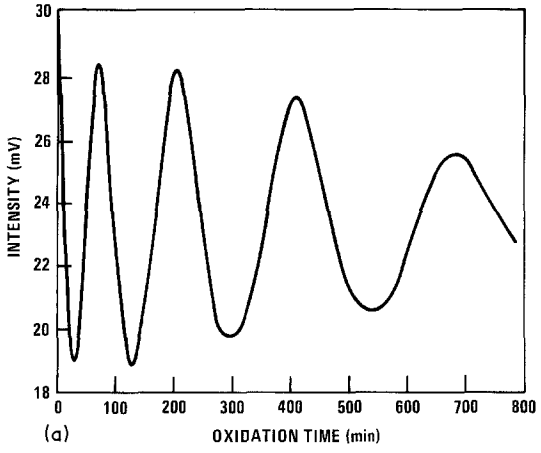

Figure 4 Normal spectral intensity of radiation emitted at 694.3 nm by a polished silicon wafer as a function of soak time at 1348° C. (a) Replot of recorded data. (b) and (c) Original recording.

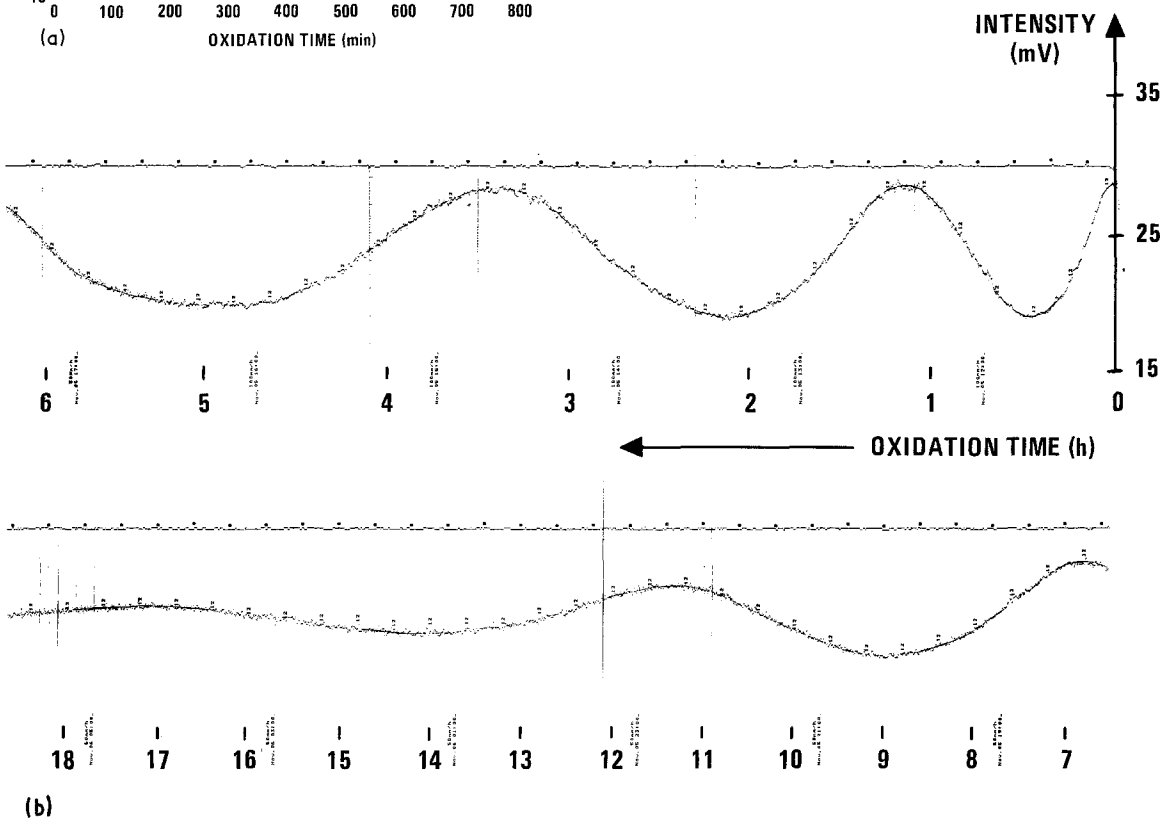

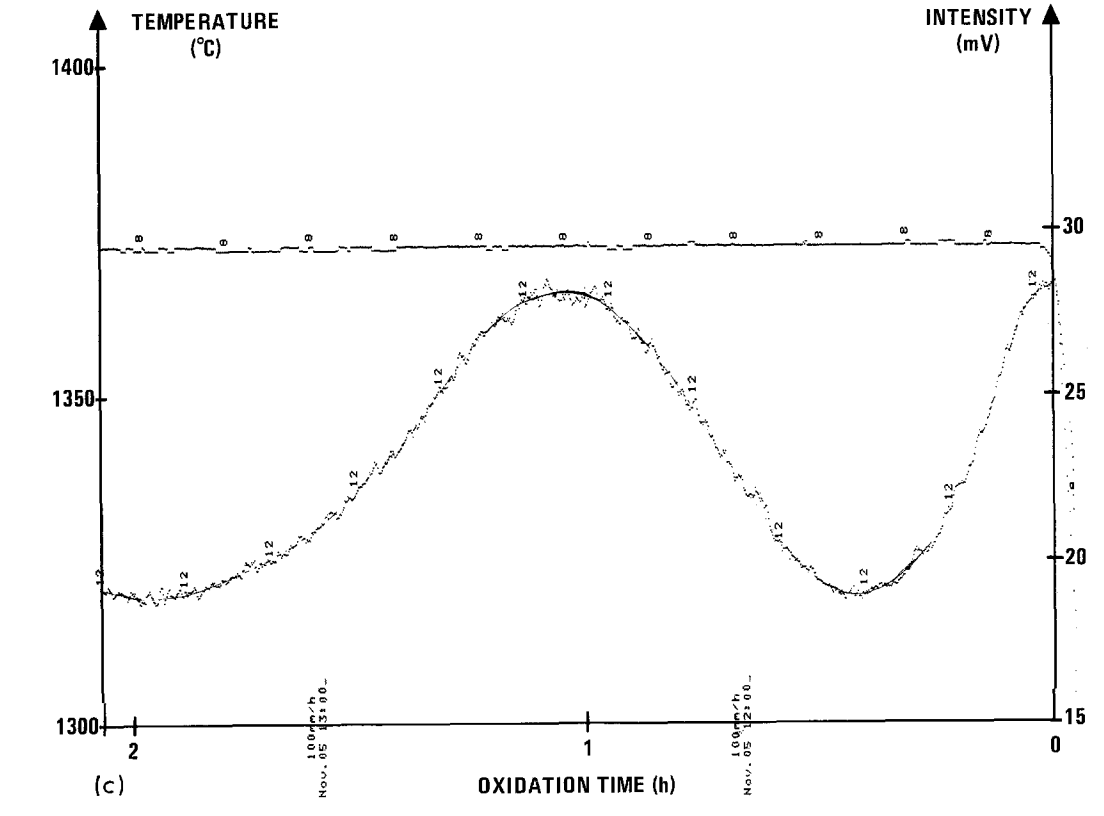

15 min. This bakeout procedure was supposed to remove moisture which is known to accelerate the oxidation of silicon. Following the bakeout, a flow of dry oxygen was established through the tube at 1 atm pressure and a rate of 15 $cm^3 min^{-1}$. Silicon samples were then rapidly heated to between 1266 and 1384° C. The sample temperatures were constant to ± 1° C over the 15 to 40 h test periods. The millivolt output of the detector, which is proportional to the intensity of radiation reaching the diode, was recorded.

4. Results and discussion

A typical curve showing the recorded intensity as a function of oxidation time is shown in Fig. 4a. This curve was obtained during an experiment in which a silicon sample was held at a temperature of 1348° C. The original recordings are shown in Figs 4b and c to give the reader an idea about the signal-to-noise ratio.

The curves recorded at other temperatures look similar to the one shown in Fig. 4. The initial ratios I_{min}/I_{max} were determined from the recorded intensities for the different experimental conditions, and all fell within the range 67 ± 1%. This is in excellent agreement with the predicted ratio of 66.9% with Equation 12.

The increase in the I_{min}/I_{max} ratio with progressing oxidation time, i.e., the disappearance of the observed intensity oscillations, is mainly due to the devitrification of the silica film into cristobalite. At higher temperatures the devitrification occurs faster, so that the film growth can be monitored up to a certain thickness only. For example, at 1348° C, we see in Fig. 4 that the oscillations have disappeared (i.e., I_{min}/I_{max} = 100%) at roughly t = 20 h corresponding to d = 1.4 μm, while at 1266° C, I_{min}/I_{max} increases from 67% at t = 0 to 75% at t = 33 h, which again corresponds to d = 1.4 μm. Other factors contribute to the decrease in oscillation amplitude as well: The finite bandwidth of the interference filter, any roughening of the silicon surface during oxidation, and any absorption taking place in the silica film (we have no absolute proof that it remains fully transparent to temperatures as high as 1384° C).

While Fig. 2 shows an initial rise in the calculated emittance, we see an initial drop in recorded intensity in Fig. 4. This is explained by the fact that a thin silica film is already formed during heat-up, i.e., before the sample reached a temperature of 1348° C. This leaves the question whether the maximum we observe in Fig. 4 at approximately t = 0 corresponds to m = 0 or 1 or 2 . . . in Equations 14 and 16. To obtain an answer to this crucial question, a sample was heated to 1350° C in an atmosphere of argon. The furnace was then quickly evacuated and back-filled with oxygen. Surprisingly, no fluctuations were observed at all. A visual examination of the sample showed that it had lost its highly reflective character. Scanning electron microscopy revealed the presence of small craters in the surface. Obviously, the sample had been severely attacked in the argon atmosphere by active oxidation, i.e., silicon reacted with oxygen impurities in the argon to form gaseous SiO instead of the protective silica film. This type of attack is observed at low oxygen

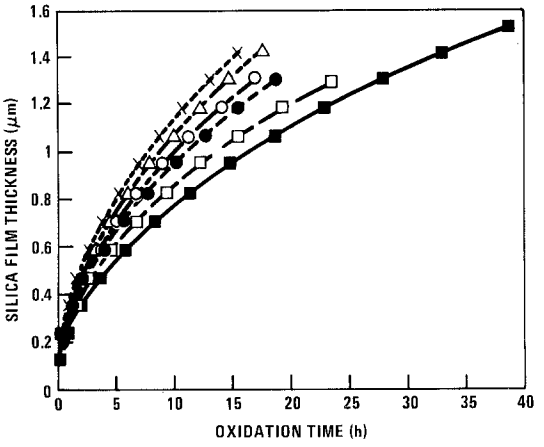

Figure 5 Silica film thickness as a function of oxidation time for six different temperatures. (■) 1266° C, (□) 1297° C, (●) 1331° C, (○) 1348° C, (△) 1366° C, (x) 1384° C.

pressures as discussed by Wagner [15]. To decrease the effect of active oxidation, another sample was heated in argon to a lower temperature of 1266° C. Immediately after reaching this temperature, the furnace was quickly evacuated and back-filled with oxygen. Now an initially rising intensity was recorded, just as predicted in Fig. 2. While an exact determination of β_{23} for 1266° C was not possible from this experiment, it can be said that it is probably close to zero, or a few degrees at most. The oxidation data obtained at 1266° C suggest that the initial maximum at about t = 0 in Fig. 4 actually corresponds to m = 0 in Equations 14 and 16.

For a plot of silica film thickness against oxidation time one has to take into account the film growth which occurs during heating to the soak temperature. This has been done in an approximative way by defining an effective oxidation time (x-axis in Figs 5, 6 and 7) as soak time at soak temperature (x-axis in Fig. 4) plus 15 min. This correction is somewhat arbitrary, but best reflects the high heating rates of the $MoSi_2$ furnace. Fortunately, for oxidation times above 5 h, this correction loses its significance, as it amounts to less than 5% of soak time. For very short soak times, however, it becomes practically impossible to determine initial oxidation rates due to film growth during heating.

Similarly, an exact value for β_{23} is most important for determining the thickness of very thin films, while for thicker films, its significance is diminished. As discussed above, a β_{23} value of 8.8° has the same influence on emittance as a 5.7 nm thick film. The first maximum in the recorded $I(t)$ curves (such as in Fig. 4) occurs, according to Equation 16 for m = 0 at d = 118 nm. Compared to this thickness, 5.7 nm is negligibly small, which justifies the use of Equations 15 and 16 for determination of the film thickness from the extrema in the recorded $I(t)$ curves.

The so determined silica film thickness is plotted as function of oxidation time for the six different test temperatures in Fig. 5. To determine whether the growth kinetics obey the parabolic law

$$d^2 = Kt \qquad (17)$$

with K as the rate constant, the data of Fig. 5 were

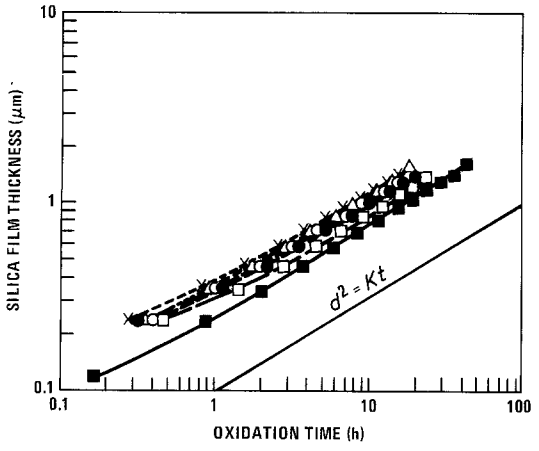

Figure 6 Double logarithmic plot of silica film thickness as a function of oxidation time for six different temperatures. (■) 1266° C, (□) 1297° C, (●) 1331° C, (○) 1348° C, (△) 1366° C, (x) 1384° C.

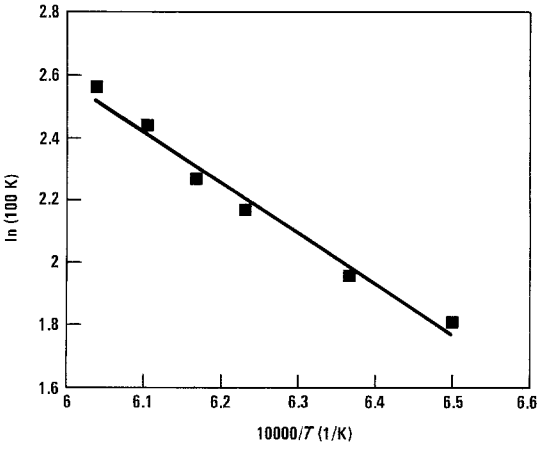

Figure 8 Activation energy for silicon oxidation in dry oxygen in the temperature range 1266 to 1384° C. $d^2 = Kt$, $K = K_0 \exp(-Q/RT)$, $Q = 135\,\mathrm{kJ\,mol^{-1}}$.

plotted on a double-logarithmic scale in Fig. 6. From this plot, an exponent of 2.02 was obtained for $T = 1266°$ C, and 2.06 for all the other temperatures. Considering the experimental uncertainties it is safe to conclude that parabolic film growth occurred over the investigated temperature range. Unfortunately, as discussed above, initial growth rates could not be determined.

A plot of the square of silica film thickness against oxidation time is shown in Fig. 7. From this figure, the parabolic rate constants K were determined for the different temperatures. A plot of ln K against $1/T$ in Fig. 8 yielded an activation energy for silicon oxidation of $135\,\mathrm{kJ\,mol^{-1}}$. This value is in good agreement with data reported in the literature [1].

5. Summary

The growth of a silica film on a polished silicon surface leads to fluctuations in the spectral emittance of an isothermally oxidized sample. These fluctuations are most pronounced at a wavelength where the silica film is fully transparent. If the normally emitted spectral radiation is monitored during isothermal oxidation of an initially bare silicon substrate, the thickness of the silica film can be determined from the extrema in the recorded intensity against time curve. The accuracy of the so obtained film thickness depends on the exact knowledge of the optical properties (n, k) of silicon and silica at the oxidation temperature and wavelength of the interference filter.

The here presented optical method has essentially three limitations: First, it is a dynamic method, and therefore does not allow the measurement of the thickness of a silica film on a silicon substrate *per se*. Second, as a sample surface does not remain completely isothermal during oxidation, but rather fluctuates somewhat in temperature due to convective currents in the furnace tube, the recorded $I(t)$ curves (Fig. 4) exhibit some noise, which requires averaging. Finally, devitrification of the silica film leads to locally differing interference conditions, which destroys the initially uniform interference in the amorphous homogeneous silica film. The main advantage of this optical technique lies in its simplicity, which makes it especially suitable for measurements at high temperatures. The method can be applied to other materials as well, e.g., it has been used to measure oxidation rates of silicon carbide and silicon nitride. The oxidation of other compounds which form a silica scale during oxidation, e.g. $MoSi_2$, could be studied with this method as well. In principle, one can study with this optical technique the oxidation of any absorbing substrate which grows a scale transparent at a wavelength where the emitted thermal energy is large enough to be detected by a photodetector.

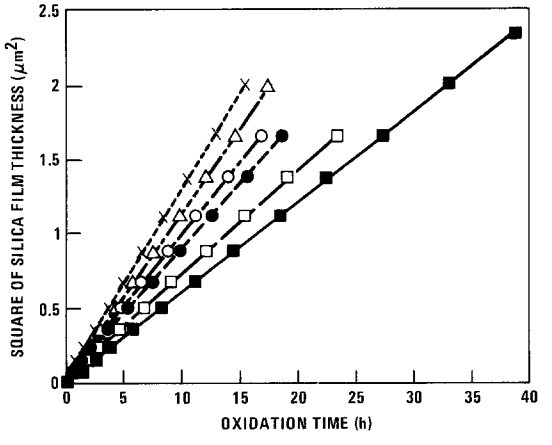

Figure 7 Square of silica film thickness as a function of oxidation time for six different temperatures. (■) 1266° C, (□) 1297° C, (●) 1331° C, (○) 1348° C, (△) 1366° C, (x) 1384° C.

Appendix A

A.1 Reflectance

An electromagnetic wave with unit amplitude is reflected from an absorbing substrate with a thin transparent film as shown in Fig. A1. The amplitude B of the reflected wave is the sum of the amplitudes of the individually reflected waves. If we introduce

$$\Delta = \beta_{23} + \alpha \qquad \text{(A1)}$$

and as

$$r_{ij} = -r_{ji} \qquad \text{(A2)}$$

write $-r_{12}$ instead of r_{21}, we obtain, omitting the

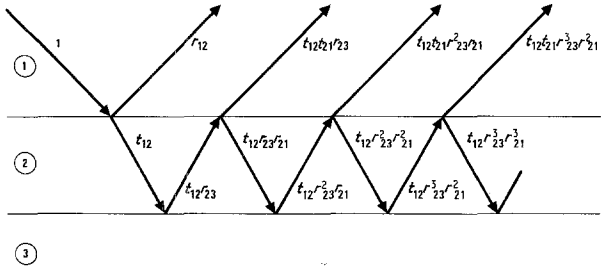

Figure A1 Reflectance of an absorbing substrate with a thin transparent film.

time-dependent factor,

$$B = r_{12} + t_{12}t_{21}r_{23}e^{i\Delta} - t_{12}t_{21}r_{12}r_{23}^2e^{i2\Delta} + \cdots$$
$$= r_{12} + \frac{t_{12}t_{21}r_{23}e^{i\Delta}}{1 + r_{12}r_{23}e^{i\Delta}} \quad \text{(A3)}$$

From conservation of energy,

$$t_{ij}t_{ji} = 1 - r_{ij}^2 \quad \text{(A4)}$$

which leads to

$$B = \frac{r_{12} + r_{23}e^{i\Delta}}{1 + r_{12}r_{23}e^{i\Delta}} \quad \text{(A5)}$$

Multiplication of B with the complex conjugate amplitude B^* yields the reflectance

$$R = BB^* = \frac{r_{12}^2 + r_{23}^2 + 2r_{12}r_{23}\cos\Delta}{1 + r_{12}^2r_{23}^2 + 2r_{12}r_{23}\cos\Delta} \quad \text{(A6)}$$

Equation A6 is identical to Equation 6 above.

A2. Emittance

Fig. A2 shows an electromagnetic wave in the (radiating) substrate with unit amplitude. Let the origin of the wave be so close to the substrate/film interface that absorption in the substrate is negligible. Then we can write for the amplitude of the emitted wave:

$$B = t_{21}t_{32}(1 + r_{21}r_{23}e^{i\Delta} + r_{21}^2r_{23}^2e^{i2\Delta} + \cdots)$$
$$= t_{21}t_{32}\frac{1}{1 + r_{12}r_{23}e^{i\Delta}} \quad \text{(A7)}$$

With Equation A4,

$$E = BB^* = \frac{1 + r_{12}^2r_{23}^2 - r_{12}^2 - r_{23}^2}{1 + r_{12}^2r_{23}^2 + 2r_{12}r_{23}\cos\Delta} \quad \text{(A8)}$$

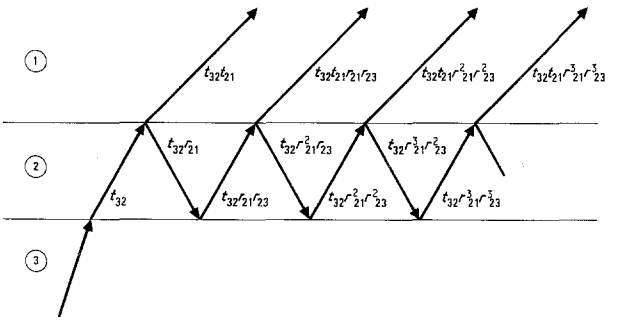

Figure A2 Emittance of an absorbing substrate with a thin transparent film.

Equation A8 can be obtained as well from $E = 1 - R$, with R from Equation A6.

References

1. B. E. DEAL and A. S. GROVE, *J. Appl. Phys.* **36** (1965) 3770.
2. E. A. TAFT, *J. Electrochem. Soc.* **132** (1985) 2486.
3. *Idem, ibid.* **131** (1984) 2460.
4. E. A. IRENE, *ibid.* **121** (1974) 1613.
5. *Idem, Appl. Phys. Lett.* **40** (1982) 74.
6. Y. J. VAN DER MEULEN, *J. Electrochem. Soc.* **119** (1972) 530.
7. Y. KAMIGAKI and Y. ITOH, *J. Appl. Phys.* **48** (1977) 2891.
8. A. G. REVESZ and R. J. EVANS, *J. Phys. Chem. Solids* **30** (1969) 551.
9. E. A. IRENE and Y. J. VAN DER MEULEN, *J. Electrochem. Soc.* **123** (1976) 1380.
10. M. A. HOPPER, R. A. CLARKE and L. YOUNG, *ibid.* **122** (1975) 1216.
11. Y. J. VAN DER MEULEN and N. C. HIEN, *J. Opt. Soc. Amer.* **64** (1974) 804.
12. M. BORN and E. WOLF, "Principles of Optics" (Pergamon, New York, 1980).
13. J. H. WRAY and J. T. NEU, *J. Opt. Soc. Amer.* **59** (1969) 774.
14. E. D. PALIK (ed), "Handbook of Optical Constants of Solids", (Academic Press, Orlando, 1985).
15. C. WAGNER, *J. Appl. Phys.* **29** (1958) 1295.

Received 20 October 1986
and accepted 24 February 1987